Phase formation and Gas sensing application of Mn substituted Lithium ferrites

R.P.Patil[a], S.B.Patil[b], A.V.Mali[c]

[a] Department of,Chemistry, M.H. Shinde Mahavidyalaya, Tisangi - 416206, MH, India

[b] Department of Physics, Krantisinh Nana Patil College Walwa,Sangli-416313 MH, India.

[c] Department of Chemistry, Yashwantrao Chavan College of Science, Karad -415124, India

Abstract:

Mangnease substituted Lithium ferrites were prepared by sol-gel route. Formation of single phase cubic spinel structure for all the compositions was confirmed from their X-ray diffraction studies. These ferrite samples existed as uniform and homogenous grain size as observed from scanning electron microscopy technique (SEM). The present work describes the gas sensing performance of the nanostructure ferrite towards H_2S, CO_2, NH_3, LPG, Ethanol, H_2 and Cl_2. It was found that the material exhibits high selectivity and sensitivity towards 50 ppm ethanol at the 250^0C temperature.

Keywords: Sol-gel method, X-ray diffraction, SEM, Gas sensing.

1.0 Introduction:

Ferrites have been studied and developed for many years because of their structural, electrical and magnetic properties that provide better applications of scientific and technological interest [1-5]. Lithium ferrite in the spinel phase, $Li_{0.5}Fe_{2.5}O_4$, has a square hysteresis loop, high magnetization and high Curie temperature. These properties are useful for technological applications such as the development of low-cost materials microwave devices. Many transition metal cations such as Mn, Cr, Co and Ti can be introduced into the lattice of the magnetic structure, which is related to a large number of applications [6-9]. Many Researchers like Wafik et. al have studied the composition dependence of discontinuous magnetization in Li-Ti ferrites [10]. Raman et. al [11] have reported the loss of lithium in Li ferrites as a result of heating above 1000^0C. Studies on electrical on Li-Co ferrites have been reported by Song et.al [12]. Microwave dielectric loss in Li-Zn ferrites has been reported by Raman et.al [13] and they observed an increase in dielectric loss with temperature. Lithium and metal substituted lithium ferrites with

possible application in the field of lithium batteries, we have developed a preparation procedure for Mn-substituted lithium ferrites system using sol-gel autocombution method. Sol-gel method is useful technique as compared to other methods, due to the better homogeneity, smaller particle size and modification of surface area.

In present investigation, an attempt is made to prepare manganese substituted lithium ferrite nanoparticles, by sol-gel auto-combustion route, which neither requires sophisticated instrument nor high sintering temperature. Their structural, electrical and magnetic properties were characterized by using x-ray diffraction (XRD), Thermal analysis (TGA-DTA) and Scanning electron microscopy(SEM) of synthesized compounds have been investigated.Various oxidizing and reducing gases were used to check the gas sensing performance of these ferrites. Different gas sensing parameters were studied in detail to express the mechanism and activity of these ferrites.

2.1. Synthesis Technique:

Polycrystalline samples having the general formula, $Li_{0.5}Fe_{2.5-x}Mn_xO_4$ ($0.0 \leq x \leq 2.5$) were synthesized by sol-gel auto-combustion method. High purity AR grade ferric nitrate, manganese nitrate, lithium nitrate and citric acid were used for synthesis. The metal nitrate solutions were mixed in the required stoichiometric ratios in minimum quantity of distilled water. The pH of the solution was maintained between 9 and 9.5 using ammonia solution. The solution mixture was slowly heated around 373K with constant stirring to obtain a fluppy mass. The precursor powder was sintered at 973K for 8 hrs, then mixed with 2 % polyvinyl alcohol as a binder and uniaxially pressed at a pressure of 8 ton/cm^2 to form the pellets.

2.2 Characterization Techniques

Thermal analysis of the different compositions of the unsintered Mn-substituted lithium ferrite system was carried out from the curves of TG-DTA. Stability of the dry citrate complexes was checked by scanning the thermograms in the temperature range of 10-1000^{o}C in static air at the flow rate of 10^0C/min. Different kinds of thermodynamic and kinetic parameters were determined from the plots of TG-DTA curves.

The phase formation of the sintered samples was confirmed by X-ray diffraction studies using Philips PW-1710 X-ray diffractometer with CuKα radiation (λ=1.54178Å).The lattice parameters were calculated for the cubic and tetragonal phase using following relations.

a) For cubic phase $a = d\,(h^2 + k^2 + l^2)^{1/2}$ ----- 1

b) For tetragonal phase $1/d^2 = h^2 + k^2 / a^2 + l^2 / c^2$ ----- 2

Where, a and c = Lattice parameters, (hkl) = Miller indices

d = interplanar distance

The crystallite size of sintered ferrites was calculated from the full width at half maxima of the most intense (311) peak by using Scherrer's formula.

$$t = 0.9\lambda / \beta \cos\theta \quad \text{-------} \quad 3$$

Where, symbols have their usual meaning.

The X-ray density was calculated according to the formula

$$dx = 8M/Na^3 \quad \text{--------} \quad 4$$

where, N = Avagadros number (6.023×10^{23} atom/mole)

M = Molecular weight, and

a = lattice constant which was calculated from the X-ray diffraction pattern. X-ray density is sometimes also called 'theoretical density'.

The SEM micrograph of the samples was obtained using scanning electron microscope (JEOL JSM 6360). The grain size of all the samples was calculated by cottrolls method.

Gas sensing performance of Mn-substituted lithium ferrite was tested against various oxidizing and reducing gases. The electrical resistance of a sensor in dry air is measured by Keithley Autoranging Picoammeter - Cleveland OH with use of conventional circuitry in which the sensor is connected to an external resistor at circuit voltage of 10 V (Aplab 7212 regulated power supplier). The values of device resistor are obtained by monitoring the output voltage across the load resistor. The resistance of the sensor was measured in the presence and absence of the test gas. A known amount of gas was introduced to attain the required level of its concentration. The gas sensing measurements were carried out at different operating temperatures (373 – 623 K). The gas response (S) is defined as the ratio of ΔR, i.e. the change in resistance of the sensor in air (R_a) and in presence of gas (R_g), normalized to the value of sensor resistance in air.

$$(\%)\ S = \left| R_a - R_g \right| / R_a \times 100 \quad \text{--------} \quad 5$$

3.0 Results and Discussion:

3.1. Phase Formation study

TG and DTA curves for the dried sample of $Li_{0.5}Fe_{1.5}Mn_{1.0}O_4$ sample are presented in **Fig. 1.** As shown in the figure, in the TG curve, the percent weight loss with the temperature is observed. A continuous weight loss was observed from TG curve upto 600˚ C of the sample in the formation of stable oxide compound. However DTA curves show one exothermic peak around 290^0C. At this temperature, a decomposition of mixed-metal citrate complexes by

fragmentation and thermal degradation of organic content occur and this results the formation of stable mixed-metal oxides.

X-ray powder diffraction patterns of $Li_{0.5}Fe_{1.5}Mn_{1.0}O_4$ nanoparticles sintered at different sintering temperature like 873 and 973K temperatures are shown in **Fig. 2.** X-ray diffraction data reveals that, the cubic crystalline phase is observed at 973K. On increasing the sintering temperature, the diffraction peaks become narrower and sharper, suggesting the increase in particle size and crystallinity of the samples.

The particle surface morphology was studied using Scanning Electron Microscopy technique (JEOL-JSM 6360 Microscope). The microstructure of the samples depends on the sintering temperature and substitution of manganese. The scanning electron micrographs of sintered samples at different temperatures 873, 973, 1073 and 1173K are shown in **Fig.3.** It can be seen that, the average grain size and crystallinity is increased significantly with increasing the sintering temperature and the particle size becomes more uniform at higher sintering temperature. At the sintering temperature of 973K, substantial grain growth occurs in which the ferrite grains are cubic and well crystalline in nature.

3.2. Study for the $Li_{0.5}Fe_{2.5-x}Mn_xO_4$ system

X-ray diffraction patterns of the Mn-substituted lithium ferrite samples, $Li_{0.5}Fe_{2.5-x}Mn_xO_4$ ($0.0 \leq x \leq 2.5$) are shown in **Fig. 4.** The various crystallographic parameters and indexed planes are summarized in Table. **1.0.** From Table, it can be seen that, the manganese substituted lithium ferrites are cubic in the range $0.0 \leq x \leq 1.5$ and tetragonal in the range of $2.0 \leq x \leq 2.5$. The tetragonal structure for x=2.0 and 2.5 is due to the Jahn-Teller effect of Mn^{3+} ions [14]. The lattice constant increases with substitution of manganese content upto x =1.5, there after decreases due to the tetragonal distortion. The increase in lattice constant with increase in Mn content is due to the higher ionic radii of Mn^{3+} (0.645Å) ions as compared to Fe^{3+} (0.64Å) ions. X-ray density (d_X) and bulk density (d_B) increased with increase in manganese content; it varies from 4.12 to 5.08 and 4.49 to 6.13 g/cm^3 respectively. The values of lattice constant (a), crystallite size (t) and X-ray density (dx) are summarized in **Table.1.** Porosity values of the Li-Mn ferrites lie in the range of 1.9 to 2.2.

The SEM images of Mn substituted lithium ferrites are shown in the **Fig.5.** It is observed that, the average grain size goes on increasing on substitution of Mn content. The average grain size was smaller than 0.1μm for all compositions.

3.3 Gas sensing studies

Gas sensing performance of each composition of the Mn-substituted lithium ferrite system has been tested for various oxidizing and reducing gases viz. ethanol, methanol, acetone, petrol,

LPG and ammonia gas. The response towards individual gas at elevated temperature is plotted in **Fig. 6-11.** To investigate gas-sensing properties, the crystalline nanosized Mn-substituted lithium ferrites powders were used in the form of pellets. The pellets of diameter 8 mm and thickness 2 mm were made under pressure of 5 tons using hydraulic press followed by sintering at 400 ^{0}C for 2 h. These pellets were then subjected to study their sensitivity and selectivity at the different controlled temperatures towards various gases in the dynamic setup.

The effect of Manganese substitution plays a significant role in the detection of various gases at different operating temperatures. It is notable that, Li-ferrite shows remarkable response towards LPG which goes on decreasing with increase in Manganese content. The response to these gases was observed at different operating temperatures. In case of petrol, ethanol, LPG maximum response was noticed at 250˚C. There is very little response for acetone, methanol and ammonia gas/vapours at any operating temperature.

Conclusions

Manganese substituted lithium ferrites of nanocrystalline nature were synthesized by sol-gel auto-combustion method. The system shows cubic phase for $x \leq 1.5$ and tetragonal for $x \geq 2.0$. From X-ray intensity calculations, it is noted that Mn^{3+}ions show strong preference for octahedral site. From thermal analysis (TGA-DTA) various thermokinetic parameters were calculated. Scanning electron micrographs indicated increase in grain size with increase in Mn content.Various reducing and oxidizing gases were tested for gas sensing activity of all the compositions of Li-Mn ferrites. Lithium ferrite shows remarkable response towards LPG with good selectivity and the sensitivity decreased in Mn rich lithium ferrites.

References:

[1] Ramachandran N and Biswas A B 1979 J. Solid State Chem. **30** 61–4

[2] Shirane T, Kanno R, Kawamoto Y, Takeda Y, Takano M, Kamiyama T and Izumi F 1995 Solid State Ionics **79** 227–33

[3] Tabuchi M et al 1998 J. Solid State Chem. **141** 554–61

[4] Smit J and Wijn H P J 1959 Ferrites (New York: Wiley)p 158

[5] Igarashi H and Okazaki K 1977, J. Am. Ceram. Soc. **60** 51

[6] Gadkari A B, Shinde T J and Vasambekar P N 2008 Mater. Chem. Phys. **114** 505–10

[7] Argentina G M and Baba P D 1974, IEEE Trans. Microw. Theory Tech. **22** 652–8

[8] Hankare P.P., Patil R.P., Sankpal U.B., Jadhav S.D., Lokhande P.D., Jadhav K.M., Sasikala R. **2009,** J. Solid State Chem. 182, 3217.

[9] Hankare P.P., Patil R.P., Sankpal U.B., Jadhav S.D., Mulla I.S., Jadhav K.M., Chougule B.K. 2009, J. Magn. Magn. Mater. 321, 3270.

[10] A.A.Wafik and S.A.Mazen, Physica status solidi (a), 86(1984)271.

[11] J.M.Song and J.G.Koh J.Magn magn.Mater, 152(1996)383.

[12] J.M.Song and J.G.Koh IEEE Tran.On magnetics, 32(2)(1996)411.

[13] R.Raman, V.R.K. Murthy and B. Vishvanathan J. Appl. Phys., 69 (7) (1991)4053

[14] M.M. Thackeray, W. I. F. David, D. G. Bruce, J. B. Goodenough, Mat. Res. Bull. 18 (1983) 461.

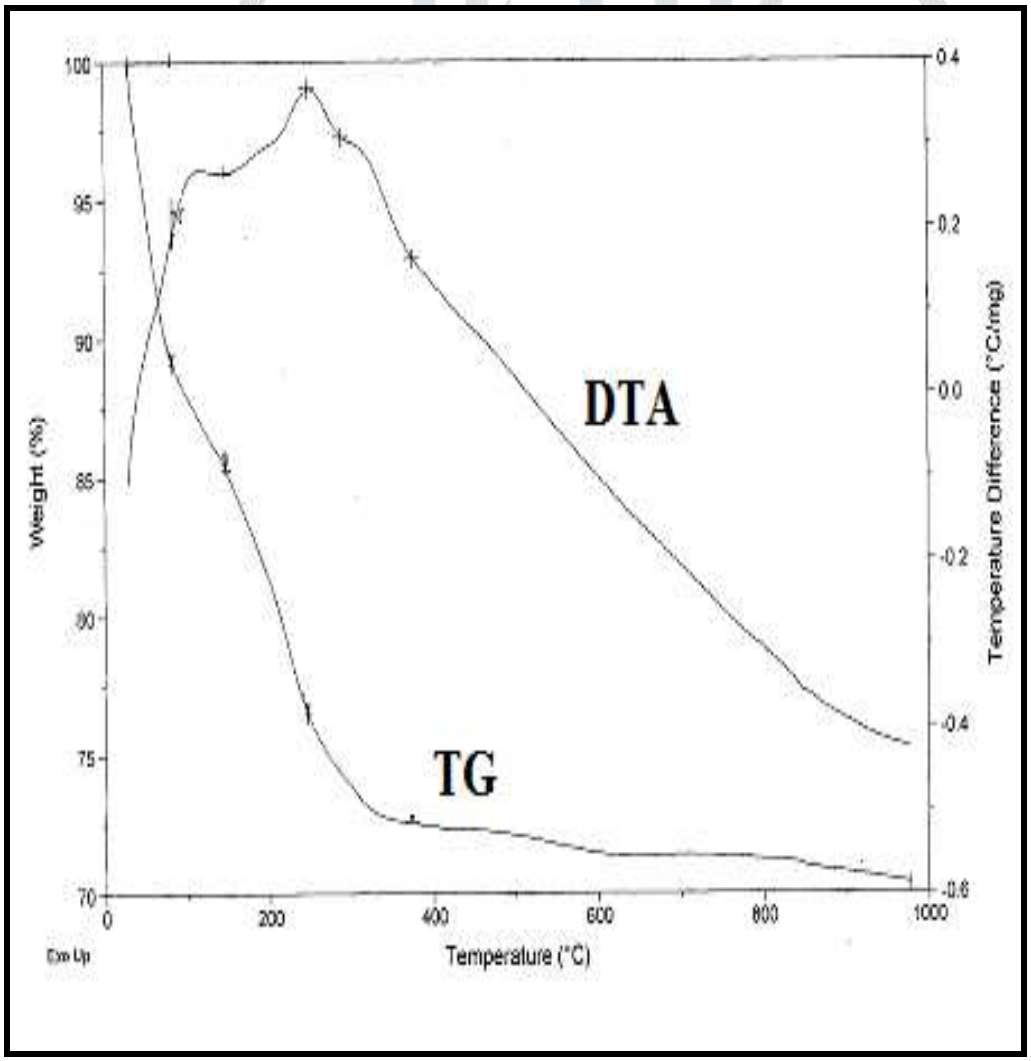

Fig. 1. TGA-DTA Spectrum for $Li_{0.5}Fe_{1.5}Mn_{1.0}O_4$

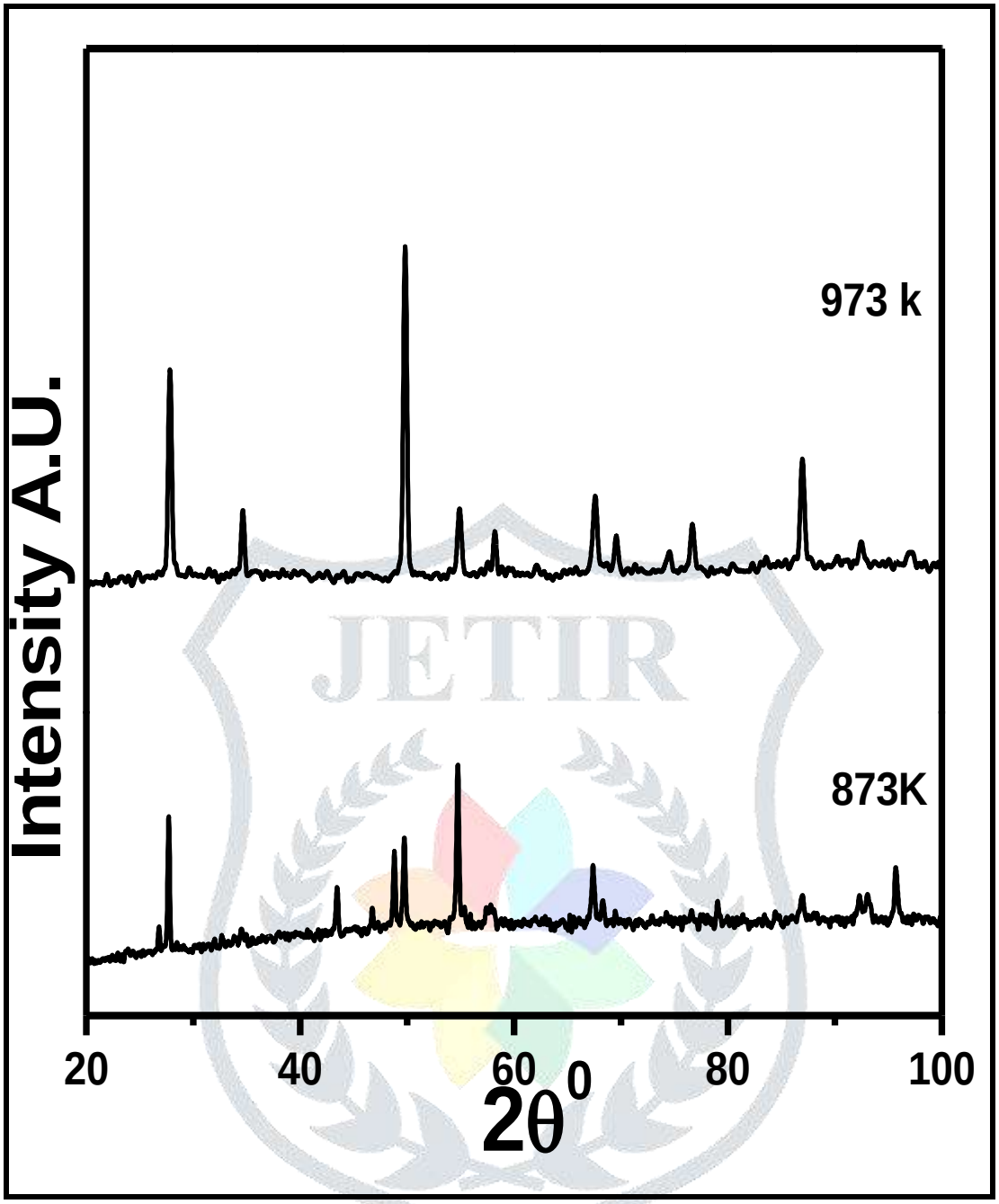

Fig.2. X-ray analysis study at different sintering Temperature

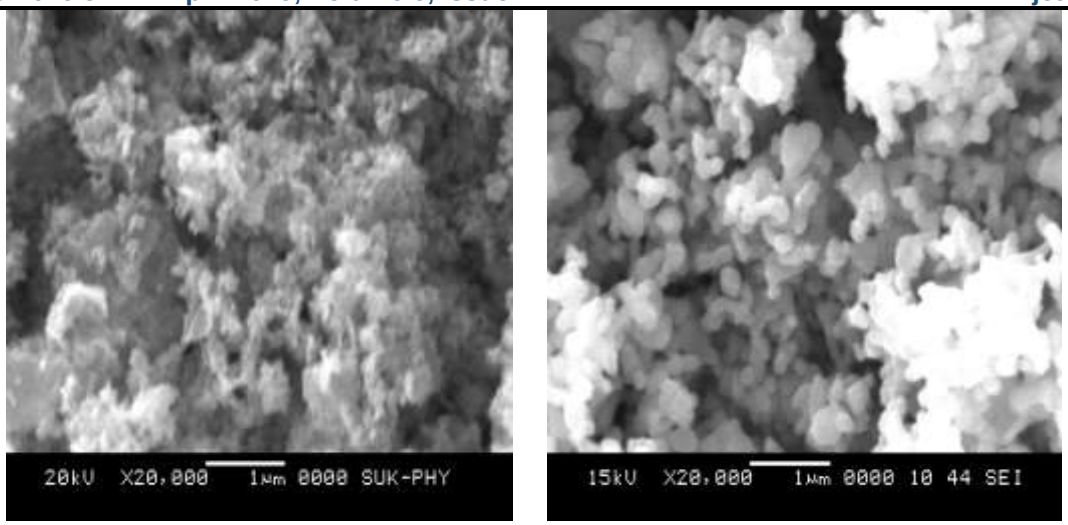

a) 873K b) 973K

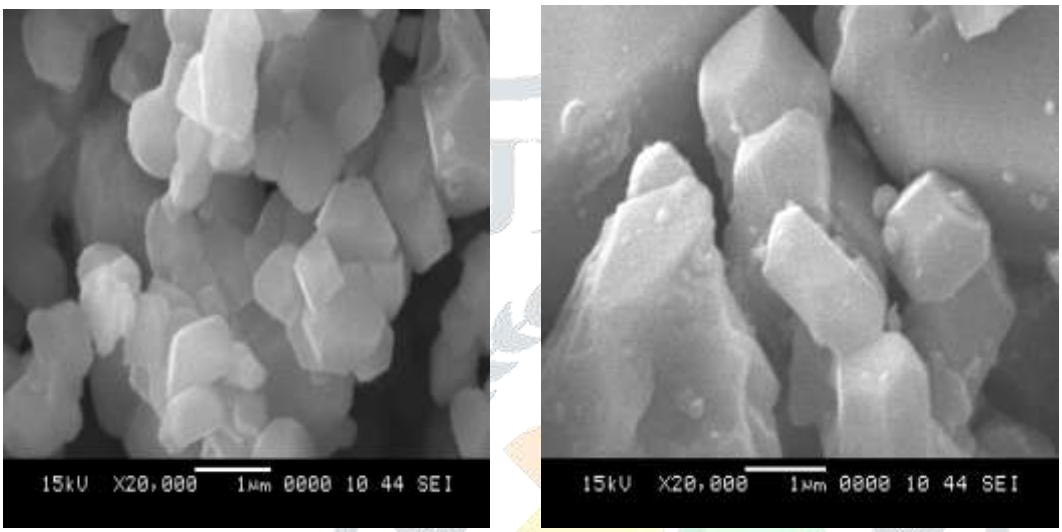

c) 1073K d) 1173K

Fig.3. SEM analysis at different sintering temperature

a) 873K, b) 973K, c) 1073K and d) 1173K

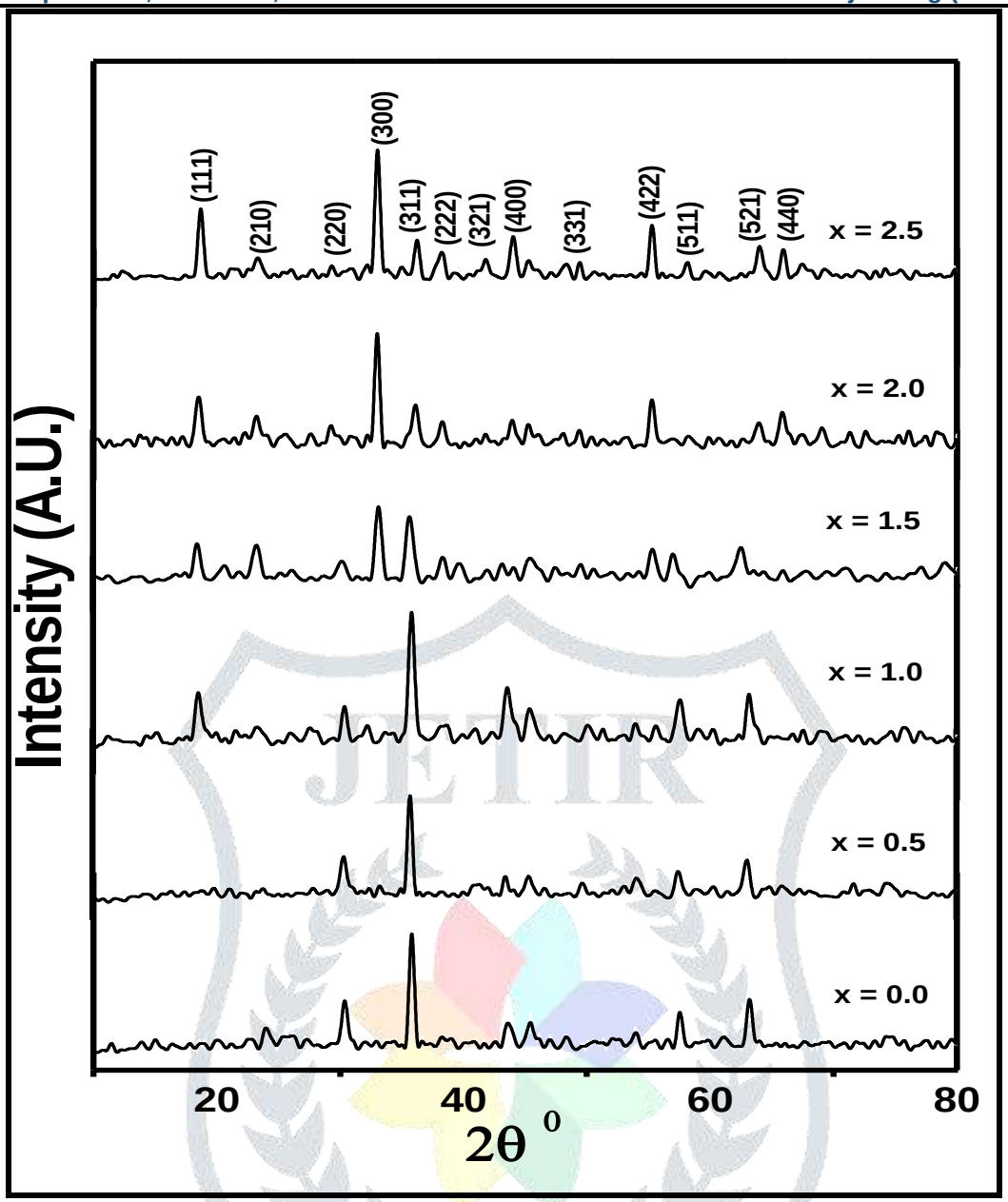

Fig.4. X-ray diffraction patterns of $Li_{0.5}Fe_{2.5-x}Mn_xO_4$ system

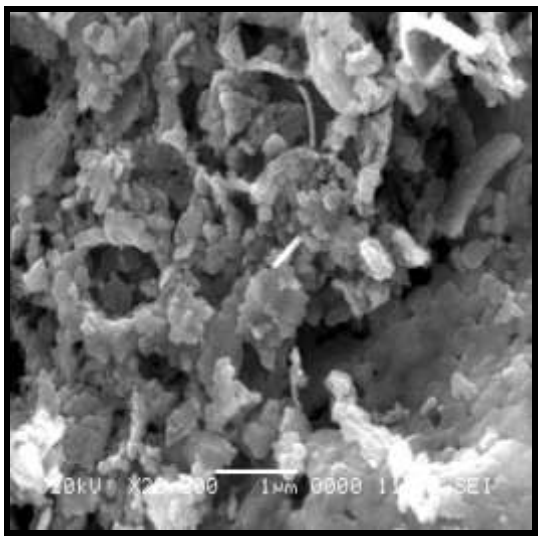

x =0.0

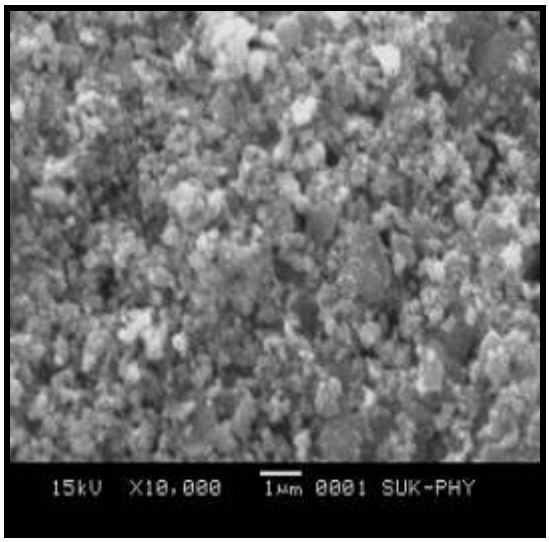

x = 0.5

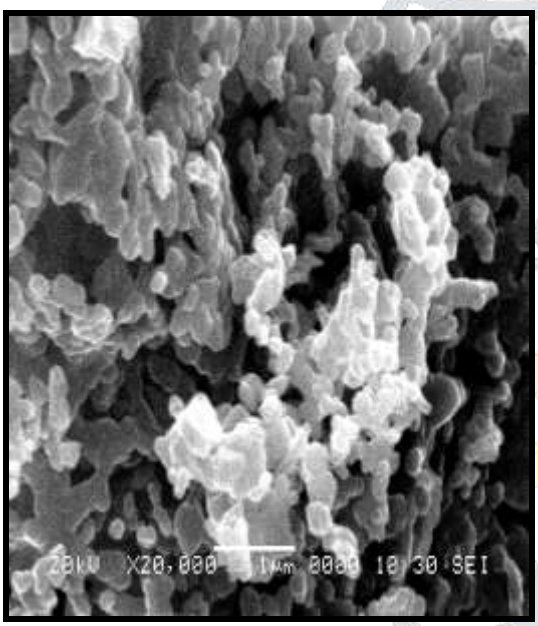

x =1.0

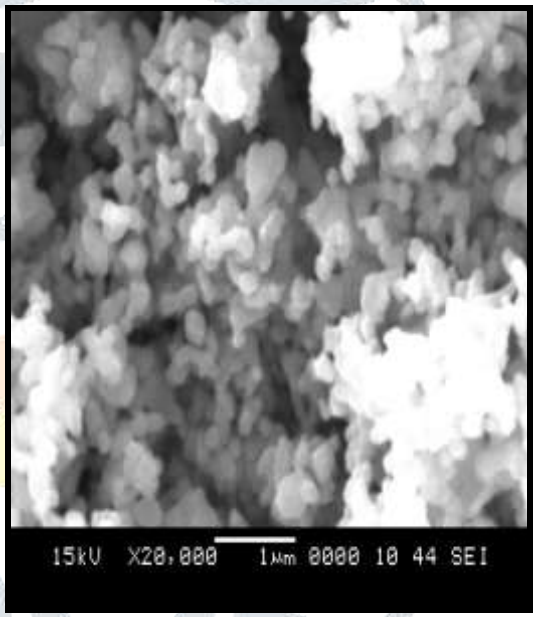

x = 1.5

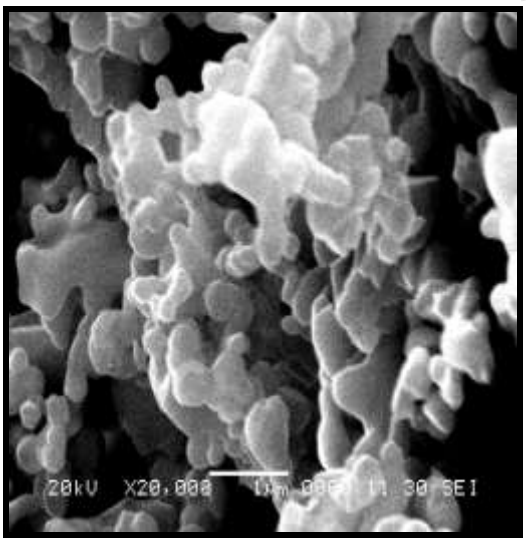

x= 2.0

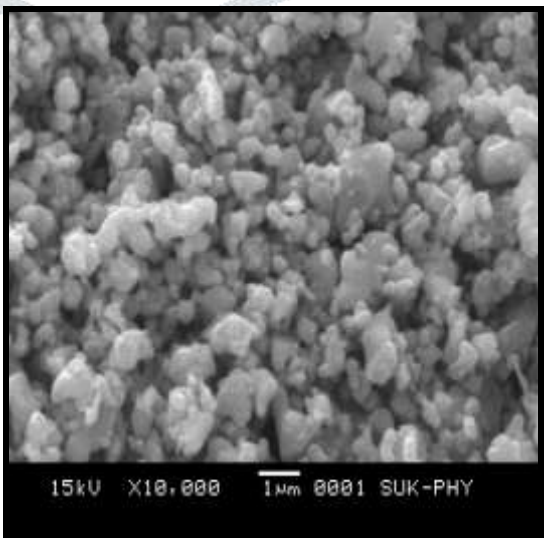

x = 2.5

Fig.5. Typical SEM images for Li $_{0.5}Fe_{2.5-x}Mn_xO_4$
x =0.0, 0.5, 1.0, 1.5, 2.0 and 2.5

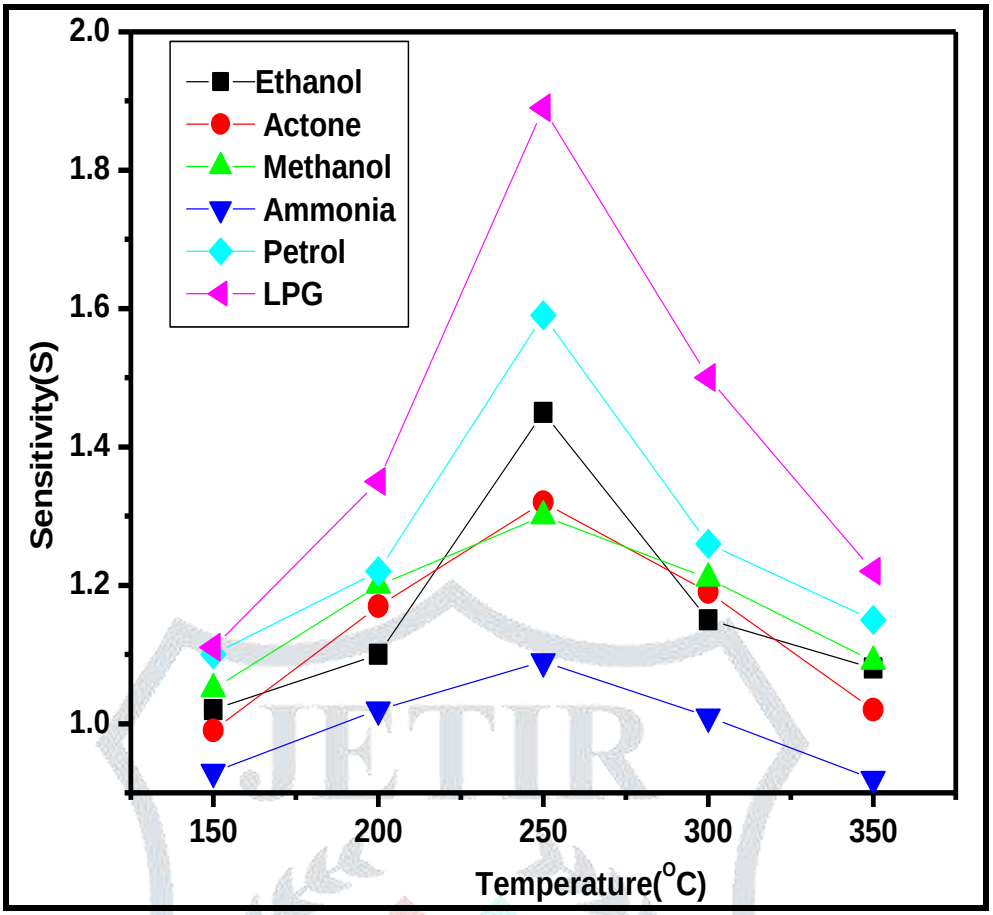

Fig. 6. Gas response of $Li_{0.5}Fe_{2.5}O_4$ towards test gases

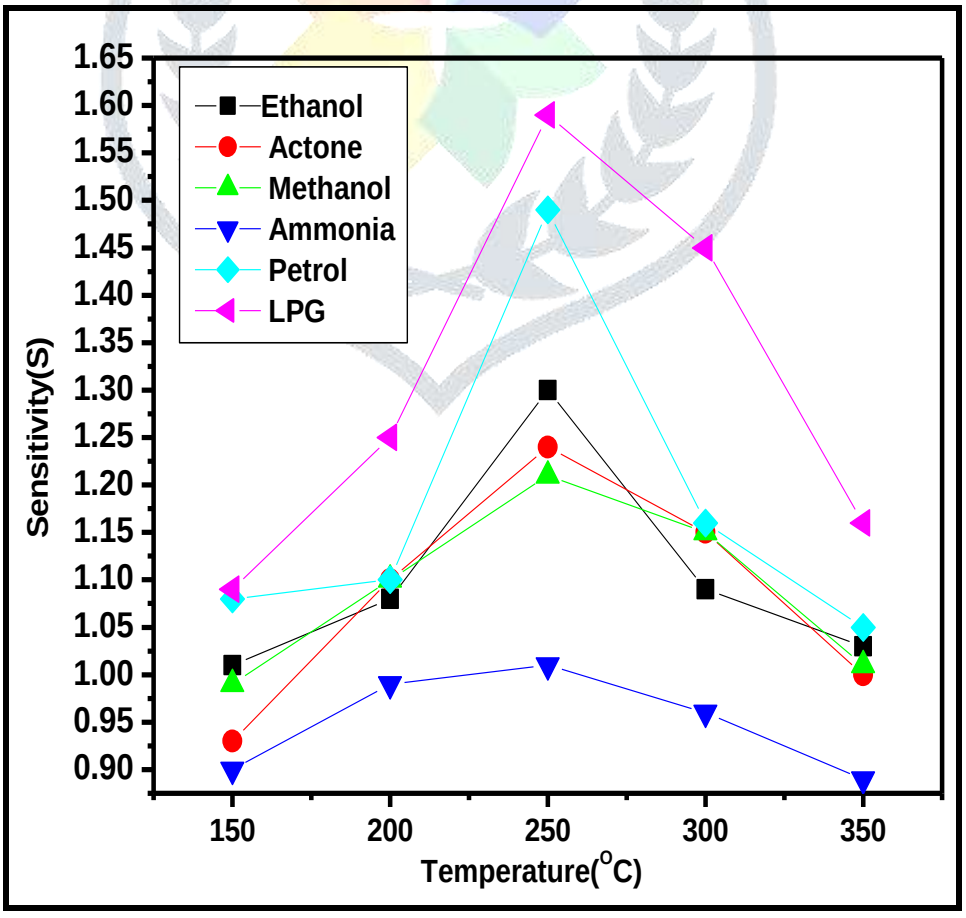

Fig. 7. Gas response of $Li_{0.5}Fe_{2.0}Mn_{0.5}O_4$ towards test gases

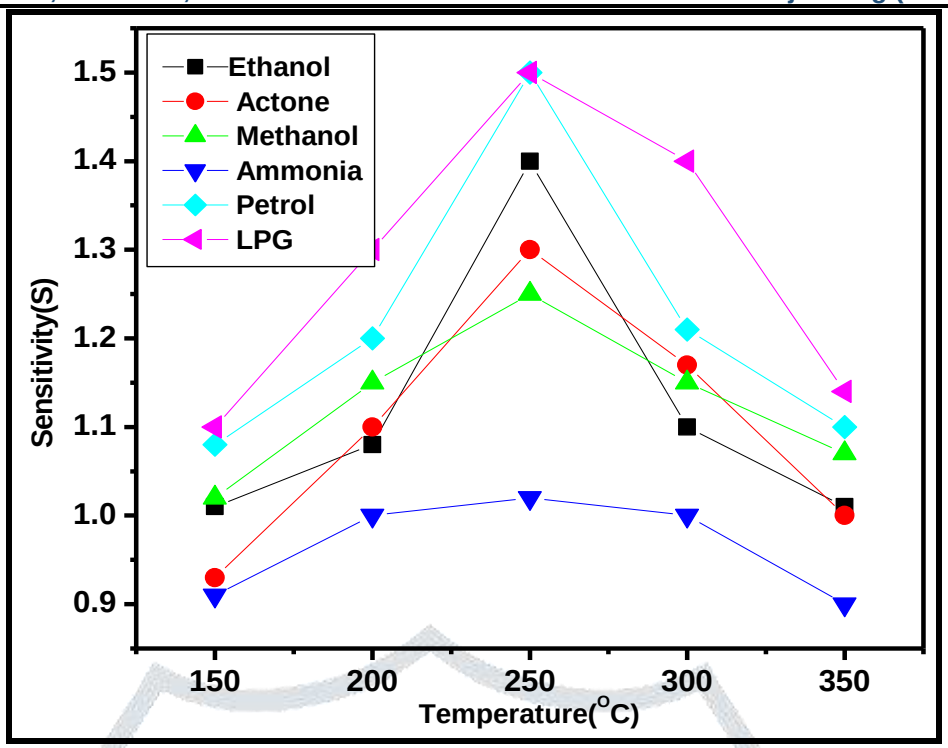

Fig. 8. Gas response of $Li_{0.5}Fe_{1.5}Mn_{1.0}O_4$ towards test gases

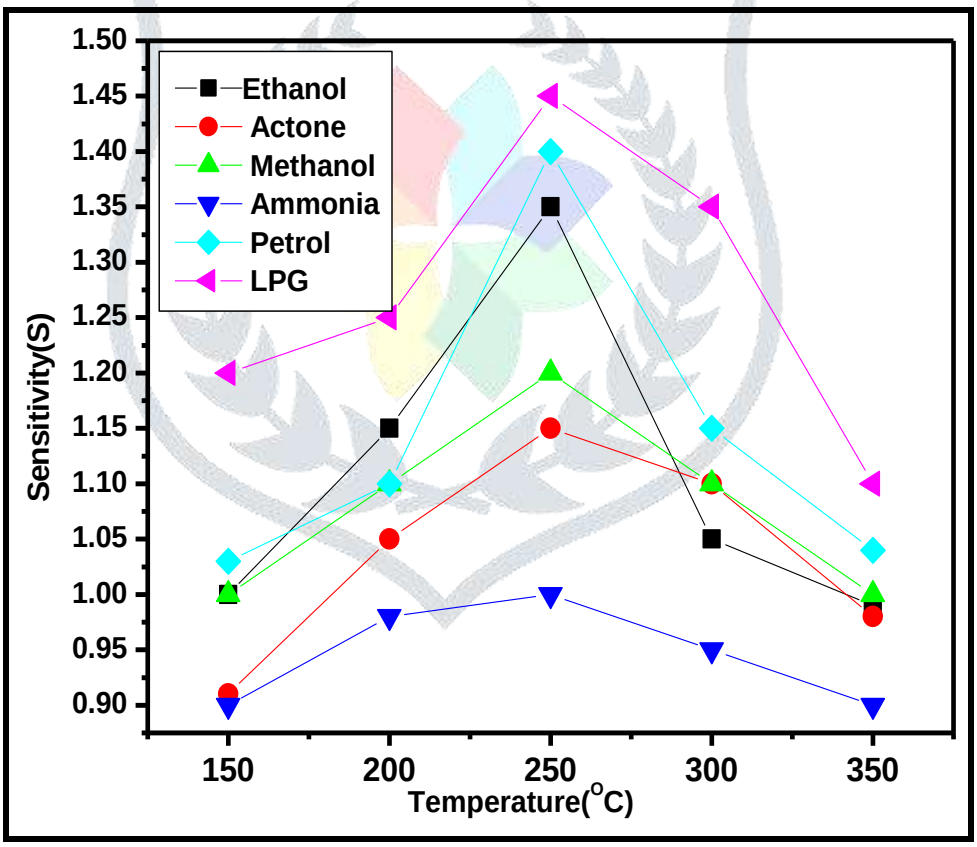

Fig. 9. Gas response of $Li_{0.5}Fe_{1.0}Mn_{1.5}O_4$ towards test gases

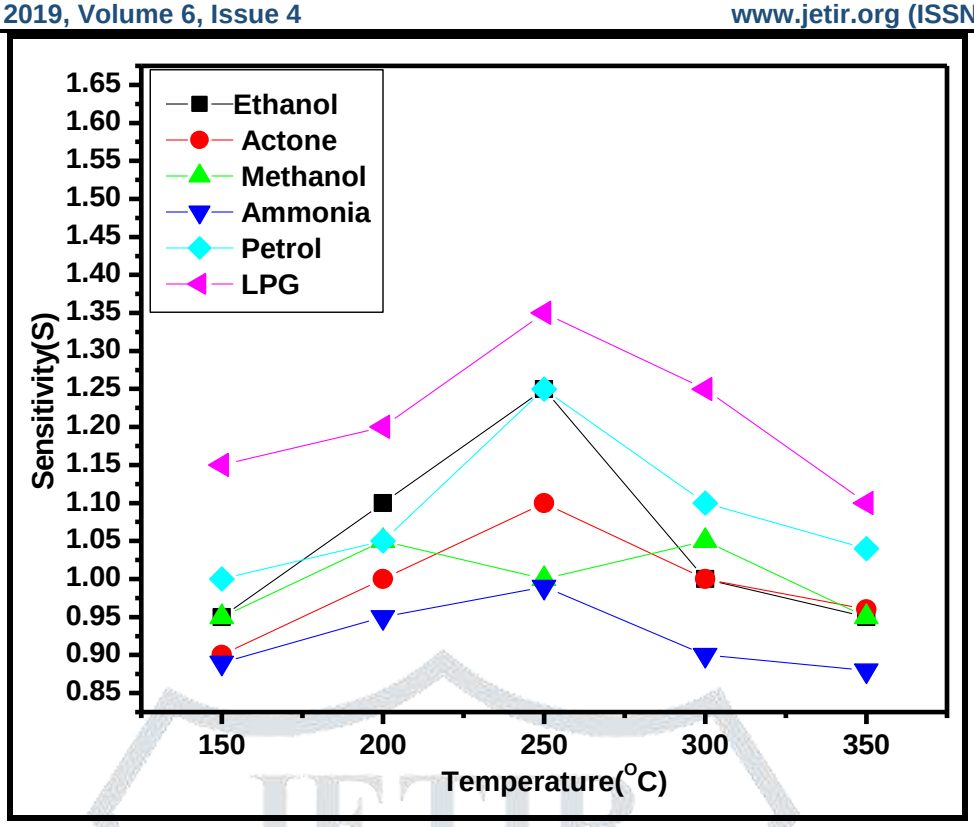

Fig. 10. Gas response of $Li_{0.5}Fe_{0.5}Mn_{2.0}O_4$ towards test gases

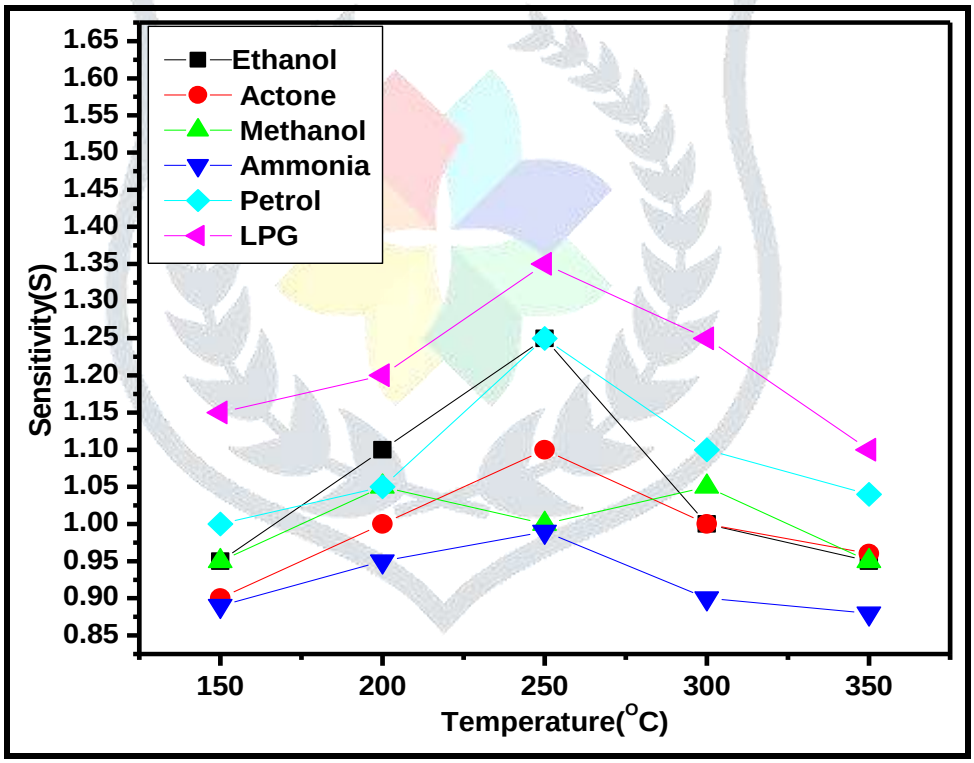

Fig. 11. Gas response of $Li_{0.5}Mn_{2.5}O_4$ towards test gases

Table.1. Data on lattice parameter, crystallite size, x-ray density and Physical density of $Li_{0.5}Fe_{2.5-x}Mn_xO_4$ ferrite samples.

Composition (x)	Lattice parameter(Å) ± 0.01	Crystallite Size(t) (nm) ± 0.01	X-ray density, (dx) (g/cm^3)	Physical density, (dx) (g/cm^3)
0.0	8.30	29.99	4.82	4.49
0.5	8.32	32.18	4.75	4.83
1.0	8.33	32.37	4.74	5.29
1.5	8.39	32.79	4.69	5.65
2.0	a = b = 5.672 c = 8.747	32.98	4.95	5.92
2.5	a = b = 5.419 c = 9.666	32.35	5.08	6.13